

SANDIA REPORT

SAND2013-7363, Rev 3: April 2014

Unlimited Release

Printed September 2013

Nonlinear Kinematics for Piezoelectricity in ALEGRA-EMMA

John A. Mitchell and Tim J. Fuller

Prepared by
Sandia National Laboratories
Albuquerque, New Mexico 87185 and Livermore, California 94550

Sandia National Laboratories is a multi-program laboratory managed and operated by Sandia Corporation, a wholly owned subsidiary of Lockheed Martin Corporation, for the U.S. Department of Energy's National Nuclear Security Administration under contract DE-AC04-94AL85000.

Approved for public release; further dissemination unlimited.



Sandia National Laboratories

Issued by Sandia National Laboratories, operated for the United States Department of Energy by Sandia Corporation.

NOTICE: This report was prepared as an account of work sponsored by an agency of the United States Government. Neither the United States Government, nor any agency thereof, nor any of their employees, nor any of their contractors, subcontractors, or their employees, make any warranty, express or implied, or assume any legal liability or responsibility for the accuracy, completeness, or usefulness of any information, apparatus, product, or process disclosed, or represent that its use would not infringe privately owned rights. Reference herein to any specific commercial product, process, or service by trade name, trademark, manufacturer, or otherwise, does not necessarily constitute or imply its endorsement, recommendation, or favoring by the United States Government, any agency thereof, or any of their contractors or subcontractors. The views and opinions expressed herein do not necessarily state or reflect those of the United States Government, any agency thereof, or any of their contractors.

Printed in the United States of America. This report has been reproduced directly from the best available copy.

Available to DOE and DOE contractors from
U.S. Department of Energy
Office of Scientific and Technical Information
P.O. Box 62
Oak Ridge, TN 37831

Telephone: (865) 576-8401
Facsimile: (865) 576-5728
E-Mail: reports@adonis.osti.gov
Online ordering: <http://www.osti.gov/bridge>

Available to the public from
U.S. Department of Commerce
National Technical Information Service
5285 Port Royal Rd
Springfield, VA 22161

Telephone: (800) 553-6847
Facsimile: (703) 605-6900
E-Mail: orders@ntis.fedworld.gov
Online ordering: <http://www.ntis.gov/help/ordermethods.asp?loc=7-4-0#online>



Nonlinear Kinematics for Piezoelectricity in *ALEGRA-EMMA*

John A. Mitchell
Multiphysics Simulation Technologies

Tim J. Fuller
Computational Structural Mechanics and Applications

Sandia National Laboratories
1515 Eubank SE
Albuquerque, NM 87185

Abstract

This report develops and documents nonlinear kinematic relations needed to implement piezoelectric constitutive models in *ALEGRA-EMMA* [5], where calculations involving large displacements and rotations are routine. Kinematic relationships are established using Gauss's law and Faraday's law; this presentation on kinematics goes beyond piezoelectric materials and is applicable to all dielectric materials. The report then turns to practical details of implementing piezoelectric models in an application code where material principal axes are rarely aligned with user defined problem coordinate axes. This portion of the report is somewhat pedagogical but is necessary in order to establish documentation for the piezoelectric implementation in *ALEGRA-EMMA*. This involves transforming elastic, piezoelectric, and permittivity moduli from material principal axes to problem coordinate axes. The report concludes with an overview of the piezoelectric implementation in *ALEGRA-EMMA* and small verification examples.

Acknowledgment

Support of this work from Erik Strack, Mike Wong, and the *Alegria* team is gratefully acknowledged. Discussions with Josh Robbins is acknowledged and appreciated. Special thanks to Tim Trucano for reviewing and commenting on a draft of this report.

Contents

| | | |
|-----|---|----|
| 1 | Introduction and Outline | 9 |
| 2 | Notation and Preliminary Development | 9 |
| | Deformation Gradient | 10 |
| | Polar Decomposition | 10 |
| | Volume Change | 10 |
| | Area Change | 10 |
| 3 | Kinematics | 11 |
| | Gauss’s Law | 11 |
| | Faraday’s Law | 12 |
| 4 | Constitutive Models for Piezoelectricity | 13 |
| 4.1 | Voight Matrix Representation | 13 |
| | 4.1.1 Elastic Moduli | 13 |
| | 4.1.2 Piezoelectric Moduli | 15 |
| 4.2 | Voight-Mandel Matrix Representation | 16 |
| | 4.2.1 Elastic Moduli | 17 |
| | 4.2.2 Piezoelectric Moduli | 18 |
| 4.3 | Voight-Mandel Matrix Transformations | 19 |
| | 4.3.1 Direction Cosine Matrix Operators | 19 |
| | 4.3.2 Moduli Transformations | 21 |
| 4.4 | Moduli Transformations: Example | 22 |
| | 4.4.1 Properties of <i>y-cut</i> Quartz | 22 |
| | 4.4.2 Transformation of <i>y-cut</i> Quartz to <i>AT-cut</i> Quartz | 24 |
| 5 | Nonlinear Kinematics for Stress and Polarization Calculations in <i>ALEGRA-EMMA</i> | 25 |
| 5.1 | Gauss’s Law for Dielectric Materials in <i>ALEGRA-EMMA</i> | 26 |
| 5.2 | State Update Algorithm for Piezoelectricity in <i>ALEGRA-EMMA</i> | 28 |
| | 5.2.1 Setup | 28 |
| | Scale User Input Moduli | 28 |
| | Transform Moduli | 29 |
| | Scale Transformed Moduli: Reverse First Step | 29 |
| | 5.2.2 Update State | 29 |
| | Compute Engineering Strain | 30 |
| | Pull Electric Field | 30 |
| | Evaluate 2nd Piola Kirchhoff Stress | 30 |
| | Evaluate Mechanical Polarization | 30 |
| | Compute Cauchy Stress | 30 |
| | De-rotate Cauchy Stress | 31 |
| | Push Permittivity Moduli | 31 |
| 5.3 | Examples | 31 |
| | 5.3.1 Rigid Rotation with Constant Electric Field | 31 |

| | | |
|-------|---|----|
| | Cauchy Stress Components | 32 |
| | Permittivity Tensor Components | 32 |
| 5.3.2 | Uniaxial Extension Plus Constant Electric Field Followed by Rigid Rotation | 33 |
| | Cauchy Stress Components | 35 |
| | Permittivity Tensor Components | 35 |
| | Mechanical polarization | 35 |
| 6 | Summary | 36 |
| | References | 39 |

List of Figures

| | | |
|---|--|----|
| 1 | Body configurations: Un-deformed and current. Lagrangian coordinates \mathbf{X} , displacement vector $\mathbf{u}(t, X)$, current coordinates $\mathbf{x}(t, \mathbf{X})$ | 10 |
| 2 | Sketch of quartz prism indicating orientation of x and y cuts; z axis is often referred to as the optical axis. | 22 |
| 3 | Schematic sketch of y -cut quartz; dotted lines indicate the optical z -axis; a) sample with respect to quartz prism; b) AT -cut sample: $\theta = 35.25^\circ$ | 23 |
| 4 | Rigid rotation with constant electric field. Material principal axes $\mathbf{g} \rightarrow (\hat{i}, \hat{j}, \hat{k})$ are initially aligned with the fixed global coordinate axes $\mathbf{G} \rightarrow (\hat{I}, \hat{J}, \hat{K})$ | 33 |
| 5 | Example from Section 5.3.1. Rigid rotation of quartz slab with constant electric field. Stress and permittivity components. Material properties used are given in Table 1..... | 34 |
| 6 | Example from Section 5.3.2. Uniaxial extension with constant electric field followed by rigid rotation. Cauchy stress. Material properties used are given in Table 1. | 36 |
| 7 | Example from Section 5.3.2. Uniaxial extension with constant electric field followed by rigid rotation. Permittivity tensor components with respect to current coordinates. Material properties used are given in Table 1..... | 37 |

List of Tables

| | | |
|---|---|----|
| 1 | Voight representation of material properties for <i>y-cut</i> quartz [7]. | 24 |
| 2 | Material/Spatial Representation of Tensors and Fields | 26 |

1 Introduction and Outline

This report documents the new piezoelectricity model implemented in *ALEGRA-EMMA* during FY2012. It covers essential kinematics, material property transformations and the algorithms implemented.

Section 2 introduces piezoelectricity and fundamental kinematics required for evaluating the model. Consistent kinematics for evaluation of the electric field and electric displacement are developed in Section 3. These relationships, applicable to all dielectric materials, are obtained using Gauss's law and Faraday's law along with basic kinematic results from Section 2. The mathematical model for piezoelectricity is described in Section 4 with an emphasis on handling anisotropy. This is particularly relevant to the practical use of piezoelectric models in application codes; implementation of these concepts in *ALEGRA-EMMA* is new. The relationship between material properties represented mathematically as tensors and material properties that are typically reported as components in Voight matrices is developed. This latter topic is not new but is documented in order to enhance transparency, understanding and usability of the implementation. Practical details of material property transformations, kinematics, and model evaluation are described in Section 5. Two simple verification type problems are also developed and documented in Section 5.

2 Notation and Preliminary Development

Piezoelectricity is a coupled theory of mechanical deformations with electric fields; strictly speaking, it is the linear couplings [7] although this report does not make this restriction in order to properly account for nonlinear kinematics. When large deformations and/or rotations are considered (as they are in *ALEGRA-EMMA*), it is very important to distinguish un-deformed coordinates from current coordinates. This section provides the minimum mathematical and notational background needed to identify and work with both sets of coordinates. The notation used here is a blend of Bonet and Wood [1] for kinematics, and Yang [7] for piezoelectricity.

The main purpose of this section is to surface key relations needed for transformations between un-deformed coordinates and current coordinates. Of particular importance are relations for areas and volumes between these two systems. The deformation gradient operator F (defined below), and its polar decomposition are central to the nonlinear kinematics. These concepts will be used in later sections of the report for transforming electric fields, polarization, stress, and strain, between un-deformed and current configurations.

A label \mathbf{X} is given to each particle in the un-deformed body. \mathbf{X} is referred to as a Lagrangian coordinate. Current coordinates \mathbf{x} are obtained through a mapping $\mathbf{x} = \phi(t, \mathbf{X})$, where ϕ is assumed to be a differentiable and invertible function of \mathbf{X} for each time t . For notational convenience, this functional relationship is simplified and denoted as $\mathbf{x} = \mathbf{x}(t, \mathbf{X})$. See Figure 1.

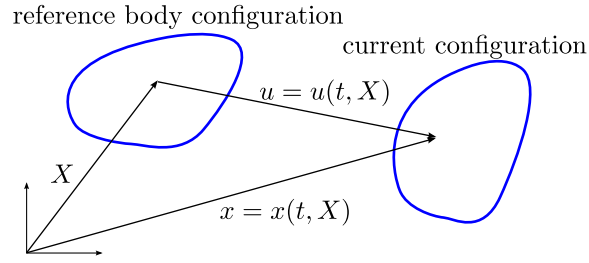


Figure 1. Body configurations: Un-deformed and current. Lagrangian coordinates \mathbf{X} , displacement vector $\mathbf{u}(t, \mathbf{X})$, current coordinates $\mathbf{x}(t, \mathbf{X})$.

Deformation Gradient

$$F = \frac{\partial \mathbf{x}}{\partial \mathbf{X}}, \quad F_{iJ} = \frac{\partial x_i}{\partial X_J}, \quad i, J = 1, \dots, 3 \quad (1)$$

Note that both \mathbf{x} and \mathbf{X} are vectors and each have 3 components; therefore F has a total of 9 components. The deformation gradient F maps an infinitesimal vector segment $d\mathbf{X}$ in the un-deformed body to an infinitesimal vector segment $d\mathbf{x}$ in the current coordinates. This is denoted by $d\mathbf{x} = F d\mathbf{X}$. In this regard, F is a two point tensor because it refers to both un-deformed and current coordinates.

Polar Decomposition The deformation gradient is multiplicatively decomposed using a rotation tensor R and either the left stretch tensor V or the right stretch tensors U .

$$F = VR = RU \quad (2)$$

Volume Change It is straight forward to establish a relationship between an infinitesimal volume dV in the un-deformed body, and the associated volume dv after deformation. The details [1, section 3.7] are omitted here.

$$\begin{aligned} dv &= |F|dV \\ &= JdV \end{aligned} \quad (3)$$

where $|F|$ denotes the determinant J of F , which is often referred to as the Jacobian.

Area Change A relation between area $d\mathbf{A}$ in the un-deformed body and the corresponding area $d\mathbf{a}$ in the deformed body is often needed. Note that **boldface** is used here to emphasize that these are vectors, i.e., each has a magnitude and an associated unit normal. Details associated with establishing this relationship are given in [1, section 3.9].

$$d\mathbf{a} = JF^{-t} d\mathbf{A} \quad (4)$$

Note that F^{-t} denotes the inverse of the transpose of F .

3 Kinematics

In this section, kinematics relevant to Gauss's and Faraday's laws are briefly introduced. These kinematics are especially relevant to *ALEGRA-EMMA* where un-deformed body coordinates must be distinguished from current coordinates. Many quantities of interest such as density, electric displacement, electric field, polarization, stress and strain have values which depend upon which configuration they are referred. Given a quantity, it is relatively easy to push or pull the quantity to either the current or un-deformed configuration respectively. This section is about exposing and developing these relations.

Gauss's Law One of the governing equations solved by *ALEGRA-EMMA* is the differential form of Gauss's law. Note that *ALEGRA-EMMA* solves Gauss's law with respect to the current configuration. With respect to the current configuration, Gauss's law reads as $\nabla \cdot (\epsilon_0 E) = \tilde{\rho}$, where E and $\tilde{\rho}$ denote the electric field and charge density respectively in the current configuration and ϵ_0 denotes vacuum permittivity. The integral form of this law states that for any closed surface, the flux of $\epsilon_0 E$ is equal to the total charge $Q = \int \tilde{\rho} dv$ enclosed by the surface [2]. In dielectric materials, the atomic lattice is idealized into a mass carrying continuum consisting of positive charges and a massless continuum consisting of negative charges. When the massless electronic continua moves with respect to the mass carrying continua, a polarization P is induced [6]. This decomposition motivates the notion of free and bound charge densities $\tilde{\rho}_f$ and $\tilde{\rho}_b$ respectively; the total charge density is taken as a sum of the free and bound charge densities $\tilde{\rho} = \tilde{\rho}_f + \tilde{\rho}_b$. Irrespective of the possible polarization mechanisms, the divergence of P induces the bound charge density: $\nabla \cdot P = -\tilde{\rho}_b$. Then, Gauss's law is written as

$$\nabla \cdot (\epsilon_0 E + P) = \tilde{\rho}_f.$$

In dielectric materials, the free charge density $\tilde{\rho}_f = 0$. This leads to the following form of Gauss's law:

$$\nabla \cdot D = 0, \tag{5}$$

where

$$D = \epsilon_0 E + P \tag{6}$$

denotes the electric displacement with respect to the current coordinates.

The integral form of Gauss's law is used to establish a relationship between \mathcal{D} , the electric displacement with respect to the un-deformed configuration, and D , which is the same but with respect to the current configuration. To establish this relationship, the surface integral in the current coordinates is transformed using (4). The current surface area is denoted by ∂a ; the corresponding area in the un-deformed configuration is denoted by ∂A .

$$\begin{aligned}
0 &= \int_{\partial a} D \cdot d\mathbf{a} \\
&= \int_{\partial A} D \cdot (JF^{-t} d\mathbf{A}) \\
&= \int_{\partial A} J(F^{-1}D) \cdot d\mathbf{A} \\
&= \int_{\partial A} \mathcal{D} \cdot d\mathbf{A}
\end{aligned}$$

The needed relationships are thus established.

$$\mathcal{D} = JF^{-1}D \quad \text{pull back} \quad (7)$$

$$D = \frac{1}{J}F\mathcal{D} \quad \text{push forward} \quad (8)$$

Faraday's Law In the integral form of Faraday's law, the electromotive force (EMF) is calculated as a path integral of the electric field. This integral is used to establish a relationship between the electric field E with respect to the current coordinates, and the electric field \mathcal{E} with respect to un-deformed coordinates. Initially, the path integral is written with respect to a loop in the current configuration using E . The deformation gradient (1) is used to pull back the integrand and thus establish a relationship between E and \mathcal{E} . The path integral using the current coordinates is denoted by ∂l ; the path integral in the un-deformed body is denoted by ∂L .

$$\begin{aligned}
EMF &= \int_{\partial l} E \cdot dl \\
&= \int_{\partial L} E \cdot (FdL) \\
&= \int_{\partial L} (F^t E) \cdot dL \\
&= \int_{\partial L} \mathcal{E} \cdot dL
\end{aligned}$$

The needed relationships are thus established.

$$\mathcal{E} = F^t E \quad \text{pull back} \quad (9)$$

$$E = F^{-t} \mathcal{E} \quad \text{push forward} \quad (10)$$

4 Constitutive Models for Piezoelectricity

Elastic, piezoelectric and permittivity material properties are 4th, 3rd, and 2nd order tensors respectively. However, notation for piezoelectricity is most commonly handled using matrices and the Voight notation. Furthermore, values for elastic and piezoelectric moduli are generally published with respect to the Voight notation. On the other hand, moduli transformations between coordinate systems are generally written in textbooks using tensor notation which tends to be less practical and cumbersome. Here, the relevant transformations of elastic, piezoelectric and permittivity moduli are written using the Voight-Mandel matrix notation which is a slightly modified version of the Voight notation. Note that the permittivity tensor is a second order tensor with components that are easily identifiable with the elements of a matrix; in the context here there is no notational difference between the Voight and Voight-Mandel representations of the permittivity tensor.

In the following two subsections, Voight and Voight-Mandel notations are briefly introduced and described for elastic and piezoelectric moduli. In the follow-on section, Voight-Mandel relations are used to transform moduli from principal material axes into the relevant problem coordinates axes. Before proceeding with the details, piezoelectric constitutive relations are summarized and denoted using the Voight matrix notation.

Piezoelectric constitutive models linearly relate strain tensor components $\{S^g\}$ and electric field components $\{\mathcal{E}^g\}$ to stress tensor components $\{T^g\}$ and electric displacement components $\{\mathcal{D}^g\}$. This relationship is denoted using the Voight matrix notation as:

$$\{T^g\} = [C^g]\{S^g\} - [e^g]^t\{\mathcal{E}^g\}, \quad \{\mathcal{D}^g\} = [e^g]\{S^g\} + [\mathcal{K}^g]\{\mathcal{E}^g\}, \quad (11)$$

where elastic moduli are denoted using the 6×6 matrix $[C^g]$, piezoelectric moduli are denoted by the 3×6 matrix $[e^g]$, and permittivity moduli are denoted using the 3×3 matrix $[\mathcal{K}^g]$. Superscripts 'g' denote values with respect to material coordinate axes; more on coordinate axes.

4.1 Voight Matrix Representation

The piezoelectric and elastic tensors are 3rd and 4th order tensors respectively. In this section, the relationship between tensor components and the Voight matrix representations of elastic and piezoelectric moduli is briefly developed and described. Superscripts 'g' and 'G', denoting material axes and global problem coordinate axes respectively, are not needed and therefore omitted.

4.1.1 Elastic Moduli

A 4th order elastic tensor maps the symmetric 2nd order strain tensor into the symmetric 2nd order stress tensor. In component form this relationship is given by

$$T_{ij} = C_{ijkl}S_{kl}, \quad (12)$$

where components of the elastic moduli tensor, stress and strain tensors are denoted by C_{ijkl} , T_{ij} , and S_{kl} respectively. In three dimensions, a 4th order tensor has $81 = 3^4$ components. However, the elastic tensor satisfies both minor and major symmetries. Minor symmetry, denoted by $C_{ijkl} = C_{ijlk}$ and $C_{ijkl} = C_{jikl}$, reduces 81 components to 36 components. Major symmetry, denoted by $C_{ijkl} = C_{klij}$ further reduces the number of independent moduli to 21. These reductions make it convenient to represent the 4th order tensor components in a symmetric 6×6 matrix. To that end, (12) is expanded and minor symmetry is exploited to relate 4th order tensor components to the Voigt notation.

$$\begin{aligned} T_{ij} &= C_{ij11}S_{11} + C_{ij22}S_{22} + C_{ij33}S_{33} \\ &+ C_{ij23}S_{23} + C_{ij32}S_{32} + C_{ij13}S_{13} + C_{ij31}S_{31} \\ &+ C_{ij12}S_{12} + C_{ij21}S_{21} \end{aligned}$$

To relate 4th order tensor components to entries in the 6×6 Voigt matrix, symmetry of the strain tensor as well as minor symmetry of the elastic tensor is used.

$$\begin{aligned} T_{ij} &= C_{ij11}S_{11} + C_{ij22}S_{22} + C_{ij33}S_{33} \\ &+ (C_{ij23} + C_{ij32})S_{23} + (C_{ij13} + C_{ij31})S_{13} + (C_{ij12} + C_{ij21})S_{12} \\ &= C_{ij11}S_{11} + C_{ij22}S_{22} + C_{ij33}S_{33} + 2C_{ij23}S_{23} + 2C_{ij13}S_{13} + 2C_{ij12}S_{12} \end{aligned}$$

$$\begin{pmatrix} T_{11} \\ T_{22} \\ T_{33} \\ T_{23} \\ T_{13} \\ T_{12} \end{pmatrix} = \begin{bmatrix} C_{1111} & C_{1122} & C_{1133} & C_{1123} & C_{1113} & C_{1112} \\ C_{2211} & C_{2222} & C_{2233} & C_{2223} & C_{2213} & C_{2212} \\ C_{3311} & C_{3322} & C_{3333} & C_{3323} & C_{3313} & C_{3312} \\ C_{2311} & C_{2322} & C_{2333} & C_{2323} & C_{2313} & C_{2312} \\ C_{1311} & C_{1322} & C_{1333} & C_{1323} & C_{1313} & C_{1312} \\ C_{1211} & C_{1222} & C_{1233} & C_{1223} & C_{1213} & C_{1212} \end{bmatrix} \begin{pmatrix} S_{11} \\ S_{22} \\ S_{33} \\ 2S_{23} \\ 2S_{13} \\ 2S_{12} \end{pmatrix}$$

In the Voigt notation, the following relations are used to represent the 4th order tensor components as entries in a 6×6 matrix. This is accomplished by relating a pair of indices to a single index. The engineering strain $2S_{ij}$, for shear shear components, i.e., $i \neq j$ is also used.

$$\begin{aligned} 11 \longrightarrow 1 : & \quad T_{11} \longrightarrow T_1, \quad S_{11} \longrightarrow S_1 \\ 22 \longrightarrow 2 : & \quad T_{22} \longrightarrow T_2, \quad S_{22} \longrightarrow S_2 \\ 33 \longrightarrow 3 : & \quad T_{33} \longrightarrow T_3, \quad S_{33} \longrightarrow S_3 \\ 23 \longrightarrow 4 : & \quad T_{23} \longrightarrow T_4, \quad 2S_{23} \longrightarrow S_4 \\ 13 \longrightarrow 5 : & \quad T_{13} \longrightarrow T_5, \quad 2S_{13} \longrightarrow S_5 \\ 12 \longrightarrow 6 : & \quad T_{12} \longrightarrow T_6, \quad 2S_{12} \longrightarrow S_6 \end{aligned} \tag{13}$$

Using the above relations, the stress-strain relationship is given in matrix notation. Note the direct correspondence of tensor components to entries in the matrix; this correspondence relies upon the

use of the engineering strain.

$$\begin{pmatrix} T_1 \\ T_2 \\ T_3 \\ T_4 \\ T_5 \\ T_6 \end{pmatrix} = \begin{bmatrix} C_{11} & C_{12} & C_{13} & C_{14} & C_{15} & C_{16} \\ \text{symm} & C_{22} & C_{23} & C_{24} & C_{25} & C_{26} \\ \text{symm} & \text{symm} & C_{33} & C_{34} & C_{35} & C_{36} \\ \text{symm} & \text{symm} & \text{symm} & C_{44} & C_{45} & C_{46} \\ \text{symm} & \text{symm} & \text{symm} & \text{symm} & C_{55} & C_{56} \\ \text{symm} & \text{symm} & \text{symm} & \text{symm} & \text{symm} & C_{66} \end{bmatrix} \begin{pmatrix} S_1 \\ S_2 \\ S_3 \\ S_4 \\ S_5 \\ S_6 \end{pmatrix} \quad (14)$$

As a row vector, components of the stress tensor are denoted as $\langle T \rangle$; similarly for the strain tensor. When represented as a column vector, components of the stress tensor are denoted by $\{T\}$; similarly for the strain tensor. Therefore, the Voight notation for Hooke's law (14) is denoted as

$$\{T\} = [C] \{S\}. \quad (15)$$

It is convenient to partition the above 6×6 elastic matrix $[C]$ into 3×3 sub-matrices along lines differentiating the normal stress/strain components from shear stress/strain components in the following way.

$$[C] = \begin{bmatrix} [C_{nn}] & [C_{ns}] \\ [C_{ns}] & [C_{ss}] \end{bmatrix} \quad (16)$$

4.1.2 Piezoelectric Moduli

The 3rd order piezoelectric tensor maps the 2nd order strain tensor into a mechanically induced polarization vector, i.e., first order tensor. In component form, this relationship is

$$dP_i = e_{ikl} S_{kl} \quad (17)$$

where components of the polarization vector, piezoelectric tensor, and strain strain tensor are denoted by dP_i , e_{ikl} , and S_{kl} . In three dimensions, a 3rd order tensor has $27 = 3^3$ components. However, the piezoelectric tensor has symmetry in the 2nd and 3rd indices, i.e. $e_{ikl} = e_{ilk}$, and this reduces the number of independent moduli from 27 to 18. With this reduction, it is feasible to represent the piezoelectric moduli as a 3×6 matrix using the Voight notation.

Similar to the procedure used for the elastic moduli, (17) is expanded.

$$\begin{aligned} dP_i &= e_{i11} S_{11} + e_{i22} S_{22} + e_{i33} S_{33} \\ &+ e_{i23} S_{23} + e_{i32} S_{32} + e_{i13} S_{13} + e_{i31} S_{31} \\ &+ e_{i12} S_{12} + e_{i21} S_{21} \end{aligned}$$

To relate this to a matrix (3×6) vector (6×1) product, symmetry of the strain tensor and piezo-

electric tensor is used.

$$\begin{aligned} dP_i &= e_{i11}S_{11} + e_{i22}S_{22} + e_{i33}S_{33} + (e_{i23} + e_{i32})S_{23} + (e_{i13} + e_{i31})S_{13} + (e_{i12} + e_{i21})S_{12} \\ &= e_{i11}S_{11} + e_{i22}S_{22} + e_{i33}S_{33} + 2e_{i23}S_{23} + 2e_{i13}S_{13} + 2e_{i12}S_{12} \end{aligned}$$

In matrix notation, the above is written as:

$$\begin{pmatrix} dP_1 \\ dP_2 \\ dP_3 \end{pmatrix} = \begin{bmatrix} e_{111} & e_{122} & e_{133} & e_{123} & e_{113} & e_{112} \\ e_{211} & e_{222} & e_{233} & e_{223} & e_{213} & e_{212} \\ e_{311} & e_{322} & e_{333} & e_{323} & e_{313} & e_{312} \end{bmatrix} \begin{pmatrix} S_{11} \\ S_{22} \\ S_{33} \\ 2S_{23} \\ 2S_{13} \\ 2S_{12} \end{pmatrix}. \quad (18)$$

The engineering strain $2S_{ij}$ is identified for shear shear components, i.e., $i \neq j$, and the above relationship is written in the following matrix notation. Note the correspondence between piezoelectric tensor components and matrix entries.

$$\begin{pmatrix} dP_1 \\ dP_2 \\ dP_3 \end{pmatrix} = \begin{bmatrix} e_{11} & e_{12} & e_{13} & e_{14} & e_{15} & e_{16} \\ e_{21} & e_{22} & e_{23} & e_{24} & e_{25} & e_{26} \\ e_{31} & e_{32} & e_{33} & e_{34} & e_{35} & e_{36} \end{bmatrix} \begin{pmatrix} S_1 \\ S_2 \\ S_3 \\ S_4 \\ S_5 \\ S_6 \end{pmatrix} \quad (19)$$

4.2 Voigt-Mandel Matrix Representation

The Voigt-Mandel representation is similar to the Voigt representation; material properties are represented in matrix form; stress and strain are represented in vector form. The difference is that components of shear strain and shear stress are scaled by $\sqrt{2}$; also, the basis used in the Voigt representation is not orthonormal and is not the same for stress and strain. On the other hand, the Voigt-Mandel representation uses the same orthonormal basis vectors for both stress and strain; this simplifies some formulas and manipulations.

A set of orthonormal basis vectors, denoted by $\mathbf{g} \rightarrow (\mathbf{g}_1, \mathbf{g}_2, \mathbf{g}_3)$, are used to construct a specialized basis \mathbf{b} for the stress and strain vectors. By way of example, the stress tensor representation is given

by:

$$\begin{aligned} \mathbf{T} &= \langle T^g \rangle \{ \mathbf{b} \} \\ &= \left\langle T_{11}^g \quad T_{22}^g \quad T_{33}^g \quad \sqrt{2}T_{23}^g \quad \sqrt{2}T_{13}^g \quad \sqrt{2}T_{12}^g \right\rangle \left\{ \begin{array}{l} \mathbf{g}_1 \otimes \mathbf{g}_1 \\ \mathbf{g}_2 \otimes \mathbf{g}_2 \\ \mathbf{g}_3 \otimes \mathbf{g}_3 \\ \frac{1}{\sqrt{2}}(\mathbf{g}_2 \otimes \mathbf{g}_3 + \mathbf{g}_3 \otimes \mathbf{g}_2) \\ \frac{1}{\sqrt{2}}(\mathbf{g}_1 \otimes \mathbf{g}_3 + \mathbf{g}_3 \otimes \mathbf{g}_1) \\ \frac{1}{\sqrt{2}}(\mathbf{g}_1 \otimes \mathbf{g}_2 + \mathbf{g}_2 \otimes \mathbf{g}_1) \end{array} \right\}. \end{aligned} \quad (20)$$

The basis vectors b_I ($I = 1, 2, \dots, 6$), are orthonormal with respect to the double dot product. For example, $b_1:b_6$ is computed as:

$$\begin{aligned} b_1:b_6 &= \mathbf{g}_1 \otimes \mathbf{g}_1 : \frac{1}{\sqrt{2}}(\mathbf{g}_1 \otimes \mathbf{g}_2 + \mathbf{g}_2 \otimes \mathbf{g}_1) \\ &= \frac{1}{\sqrt{2}}((\mathbf{g}_1 \cdot \mathbf{g}_1)(\mathbf{g}_1 \cdot \mathbf{g}_2) + (\mathbf{g}_1 \cdot \mathbf{g}_2)(\mathbf{g}_1 \cdot \mathbf{g}_1)) \\ &= \frac{1}{\sqrt{2}}((1)(0) + (0)(1)) \\ &= 0. \end{aligned} \quad (21)$$

As a second example, evaluation of $b_6:b_6$ is given by:

$$\begin{aligned} b_6:b_6 &= \frac{1}{\sqrt{2}}(\mathbf{g}_1 \otimes \mathbf{g}_2 + \mathbf{g}_2 \otimes \mathbf{g}_1) : \frac{1}{\sqrt{2}}(\mathbf{g}_1 \otimes \mathbf{g}_2 + \mathbf{g}_2 \otimes \mathbf{g}_1) \\ &= \frac{1}{2}((\mathbf{g}_1 \cdot \mathbf{g}_2)(\mathbf{g}_2 \cdot \mathbf{g}_1) + (\mathbf{g}_1 \cdot \mathbf{g}_1)(\mathbf{g}_2 \cdot \mathbf{g}_2) + (\mathbf{g}_1 \cdot \mathbf{g}_1)(\mathbf{g}_2 \cdot \mathbf{g}_2) + (\mathbf{g}_2 \cdot \mathbf{g}_1)(\mathbf{g}_1 \cdot \mathbf{g}_2)) \\ &= \frac{1}{2}((0)(0) + (1)(1) + (1)(1) + (0)(0)) \\ &= 1. \end{aligned}$$

With this representation, a Voigt-Mandel component of the stress tensor can be found by using the double dot product; $\sqrt{2}T_{12}^g = \mathbf{T} : \frac{1}{\sqrt{2}}(\mathbf{g}_1 \otimes \mathbf{g}_2 + \mathbf{g}_2 \otimes \mathbf{g}_1)$.

4.2.1 Elastic Moduli

In the Voigt-Mandel representation, the elastic 6×6 matrix $[C]$ in (16) is slightly modified to accommodate the Voigt-Mandel stress and strain components described above. The Voigt-Mandel elastic matrix, denoted as $[\tilde{C}]$, relates to the Voigt matrix $[C]$ in the following way:

$$[\tilde{C}] = \begin{bmatrix} [C_{nm}] & \sqrt{2}[C_{ns}] \\ \sqrt{2}[C_{ns}] & 2[C_{ss}] \end{bmatrix}. \quad (22)$$

The above scaling factors of $\sqrt{2}$ and 2 are established by equating stress tensor components from the Voigt representation with stress tensor components from the Voigt-Mandel representation. This is illustrated using two components $T_1 = T_{xx}$ and $T_6 = T_{xy}$; these two components establish the scaling of $[C_{ns}]$ and $[C_{ss}]$ respectively. From (14), T_1 is given by

$$T_1 = C_{11}S_1 + C_{12}S_2 + C_{13}S_3 + C_{14}(2S_{23}) + C_{15}(2S_{13}) + C_{16}(2S_{12}).$$

Similarly, the above component is evaluated using the Voigt-Mandel representation. Note that in this representation, shear stress and strain components are scaled by $\sqrt{2}$.

$$T_1 = \tilde{C}_{11}S_1 + \tilde{C}_{12}S_2 + \tilde{C}_{13}S_3 + \tilde{C}_{14}(\sqrt{2}S_{23}) + \tilde{C}_{15}(\sqrt{2}S_{13}) + \tilde{C}_{16}(\sqrt{2}S_{12})$$

The above two values for T_1 are equated; similarly, if this process is repeated for T_2 and T_3 , it is evident that $[\tilde{C}_{ns}] = \sqrt{2}[C_{ns}]$.

A similar procedure is followed for T_6 . From (14), T_6 is given by

$$T_6 = C_{16}S_1 + C_{26}S_2 + C_{36}S_3 + C_{46}(2S_{23}) + C_{56}(2S_{13}) + C_{66}(2S_{12}). \quad (23)$$

And again using the Voigt-Mandel representation; note that shear stress and strain components are scaled by $\sqrt{2}$.

$$\sqrt{2}T_6 = \tilde{C}_{16}S_1 + \tilde{C}_{26}S_2 + \tilde{C}_{36}S_3 + \tilde{C}_{46}(\sqrt{2}S_{23}) + \tilde{C}_{56}(\sqrt{2}S_{13}) + \tilde{C}_{66}(\sqrt{2}S_{12}) \quad (24)$$

Next, (23) is multiplied by $\sqrt{2}$ and then equated with (24); similarly, if this process is repeated for T_4 and T_5 , it is evident that $[\tilde{C}_{ss}] = 2[C_{ss}]$. This process uses the previously established relationship $[\tilde{C}_{ns}] = \sqrt{2}[C_{ns}]$.

4.2.2 Piezoelectric Moduli

Following a procedure similar to that for the elastic 4th order tensor, the Voigt-Mandel representation of the piezoelectric tensor is established. Expressions for the Voigt representation in (18) are used. For convenience, the Voigt representation for the mechanically induced polarization is written again.

$$dP_i = e_{i11}S_{11} + e_{i22}S_{22} + e_{i33}S_{33} + 2e_{i23}S_{23} + 2e_{i13}S_{13} + 2e_{i12}S_{12}$$

The Voigt-Mandel representation is written as:

$$dP_i = \tilde{e}_{i1}S_{11} + \tilde{e}_{i2}S_{22} + \tilde{e}_{i3}S_{33} + \tilde{e}_{i4}\sqrt{2}S_{23} + \tilde{e}_{i5}\sqrt{2}S_{13} + \tilde{e}_{i6}\sqrt{2}S_{12}.$$

Equating the above two relations for the mechanically induced polarization establishes the appropriate scaling of piezoelectric tensor components for use in the Voigt-Mandel matrix representa-

tion.

$$\begin{pmatrix} dP_1 \\ dP_2 \\ dP_3 \end{pmatrix} = \begin{bmatrix} e_{111} & e_{122} & e_{133} & \sqrt{2}e_{123} & \sqrt{2}e_{113} & \sqrt{2}e_{112} \\ e_{211} & e_{222} & e_{233} & \sqrt{2}e_{223} & \sqrt{2}e_{213} & \sqrt{2}e_{212} \\ e_{311} & e_{322} & e_{333} & \sqrt{2}e_{323} & \sqrt{2}e_{313} & \sqrt{2}e_{312} \end{bmatrix} \begin{pmatrix} S_{11} \\ S_{22} \\ S_{33} \\ \sqrt{2}S_{23} \\ \sqrt{2}S_{13} \\ \sqrt{2}S_{12} \end{pmatrix} \quad (25)$$

4.3 Voigt-Mandel Matrix Transformations

4.3.1 Direction Cosine Matrix Operators

For modeling purposes, it is necessary to relate material axes to model coordinate axes since material axes are in general different from problem coordinate axes. This section describes the relevant transformations for elastic, piezoelectric, and permittivity matrices.

Material properties are typically known with respect to material principal axes $\mathbf{g} \rightarrow (\mathbf{g}_1, \mathbf{g}_2, \mathbf{g}_3)$, where \mathbf{g}_i for $i = 1, 2, 3$, denote orthonormal vectors. In practice, material principal axes are rarely coincident with the problem coordinates axes, $\mathbf{G} \rightarrow (\mathbf{G}_1, \mathbf{G}_2, \mathbf{G}_3)$, and it is necessary to transform material properties from one basis to the other. This is accomplished using a standard 3×3 direction cosine matrix $[a^{Gg}]$, the columns of which represent basis vectors of \mathbf{g} expressed as a linear combination of the basis vectors for \mathbf{G} . This matrix is given by:

$$[a^{Gg}] = \begin{bmatrix} \mathbf{G}_1 \cdot \mathbf{g}_1 & \mathbf{G}_1 \cdot \mathbf{g}_2 & \mathbf{G}_1 \cdot \mathbf{g}_3 \\ \mathbf{G}_2 \cdot \mathbf{g}_1 & \mathbf{G}_2 \cdot \mathbf{g}_2 & \mathbf{G}_2 \cdot \mathbf{g}_3 \\ \mathbf{G}_3 \cdot \mathbf{g}_1 & \mathbf{G}_3 \cdot \mathbf{g}_2 & \mathbf{G}_3 \cdot \mathbf{g}_3 \end{bmatrix} = \begin{bmatrix} a_{11}^{Gg} & a_{12}^{Gg} & a_{13}^{Gg} \\ a_{21}^{Gg} & a_{22}^{Gg} & a_{23}^{Gg} \\ a_{31}^{Gg} & a_{32}^{Gg} & a_{33}^{Gg} \end{bmatrix} \quad (26)$$

where columns represent material axes with respect to the problem coordinates axes. Using $[a^{Gg}]$, vector components with respect to the \mathbf{g} basis can easily be transformed to components with respect to the \mathbf{G} basis. As an example, suppose that the following representation of the electric field is given.

$$\begin{aligned} \mathbf{E} &= \langle E^g \rangle \{g\} \\ &= E_1^g \mathbf{g}_1 + E_2^g \mathbf{g}_2 + E_3^g \mathbf{g}_3 \end{aligned}$$

Then components with respect to the \mathbf{G} basis can be computed by:

$$\begin{aligned} E_i^G &= \mathbf{E} \cdot \mathbf{G}_i \\ &= (\mathbf{G}_i \cdot \mathbf{g}_1) E_1^g + (\mathbf{G}_i \cdot \mathbf{g}_2) E_2^g + (\mathbf{G}_i \cdot \mathbf{g}_3) E_3^g \\ &= a_{ij}^{Gg} E_j^g \quad \text{sum on } j = 1, 2, 3 \end{aligned}$$

Utilizing matrix notation, components of the electric field transform as

$$\{E^G\} = [a^{Gg}] \{E^g\}. \quad (27)$$

Tensors using the Voight-Mandel representation are transformed in a similar way. The Voight-Mandel basis defined in (20) is established using the material basis \mathbf{g} and problem coordinate basis \mathbf{G} ; these two bases are denoted by \mathbf{b} and \mathbf{B} respectively. For completeness, components of \mathbf{B} are similarly defined (see (20)):

$$\{\mathbf{B}\} = \left\{ \begin{array}{c} \mathbf{G}_1 \otimes \mathbf{G}_1 \\ \mathbf{G}_2 \otimes \mathbf{G}_2 \\ \mathbf{G}_3 \otimes \mathbf{G}_3 \\ \frac{1}{\sqrt{2}}(\mathbf{G}_2 \otimes \mathbf{G}_3 + \mathbf{G}_3 \otimes \mathbf{G}_2) \\ \frac{1}{\sqrt{2}}(\mathbf{G}_1 \otimes \mathbf{G}_3 + \mathbf{G}_3 \otimes \mathbf{G}_1) \\ \frac{1}{\sqrt{2}}(\mathbf{G}_1 \otimes \mathbf{G}_2 + \mathbf{G}_2 \otimes \mathbf{G}_1) \end{array} \right\} \quad (28)$$

The relevant 6×6 transformation matrix $[A^{Gg}]$ is given by dotting each component of \mathbf{B} with each component of \mathbf{b} . Conceptually, each component of \mathbf{b} is expressed as a linear combination of the basis vectors \mathbf{B}_I for $I = 1, 2, 3, 4, 5, 6$. The transformation matrix $[A^{Gg}]$ is given as

$$[A^{Gg}] = \begin{bmatrix} \mathbf{B}_1 : \mathbf{b}_1 & \mathbf{B}_1 : \mathbf{b}_2 & \mathbf{B}_1 : \mathbf{b}_3 & \mathbf{B}_1 : \mathbf{b}_4 & \mathbf{B}_1 : \mathbf{b}_5 & \mathbf{B}_1 : \mathbf{b}_6 \\ \mathbf{B}_2 : \mathbf{b}_1 & \mathbf{B}_2 : \mathbf{b}_2 & \mathbf{B}_2 : \mathbf{b}_3 & \mathbf{B}_2 : \mathbf{b}_4 & \mathbf{B}_2 : \mathbf{b}_5 & \mathbf{B}_2 : \mathbf{b}_6 \\ \mathbf{B}_3 : \mathbf{b}_1 & \mathbf{B}_3 : \mathbf{b}_2 & \mathbf{B}_3 : \mathbf{b}_3 & \mathbf{B}_3 : \mathbf{b}_4 & \mathbf{B}_3 : \mathbf{b}_5 & \mathbf{B}_3 : \mathbf{b}_6 \\ \mathbf{B}_4 : \mathbf{b}_1 & \mathbf{B}_4 : \mathbf{b}_2 & \mathbf{B}_4 : \mathbf{b}_3 & \mathbf{B}_4 : \mathbf{b}_4 & \mathbf{B}_4 : \mathbf{b}_5 & \mathbf{B}_4 : \mathbf{b}_6 \\ \mathbf{B}_5 : \mathbf{b}_1 & \mathbf{B}_5 : \mathbf{b}_2 & \mathbf{B}_5 : \mathbf{b}_3 & \mathbf{B}_5 : \mathbf{b}_4 & \mathbf{B}_5 : \mathbf{b}_5 & \mathbf{B}_5 : \mathbf{b}_6 \\ \mathbf{B}_6 : \mathbf{b}_1 & \mathbf{B}_6 : \mathbf{b}_2 & \mathbf{B}_6 : \mathbf{b}_3 & \mathbf{B}_6 : \mathbf{b}_4 & \mathbf{B}_6 : \mathbf{b}_5 & \mathbf{B}_6 : \mathbf{b}_6 \end{bmatrix}.$$

The above matrix can be partitioned into 3×3 matrices whose components depend upon components of $[a^{Gg}]$:

$$[A^{Gg}] = \begin{bmatrix} [A_{nn}^{Gg}] & [A_{ns}^{Gg}] \\ [A_{sn}^{Gg}] & [A_{ss}^{Gg}] \end{bmatrix}, \quad (29)$$

where components of the above sub-matrices are given by:

$$[A_{nn}^{Gg}] \longrightarrow A_{IJ}^{Gg} = a_{ij}a_{ij} \quad \text{for } \begin{cases} I = 1, 2, 3; i = 1, 2, 3 \\ J = 1, 2, 3; j = 1, 2, 3 \end{cases} \quad (30)$$

$$[A_{ns}^{Gg}] \longrightarrow A_{IJ}^{Gg} = \sqrt{2}a_{ij}a_{ik} \quad \text{for } \begin{cases} I = 1, 2, 3; i = 1, 2, 3 \\ J = 4, 5, 6; (j, k) = (2, 3), (1, 3), (1, 2) \end{cases} \quad (31)$$

$$[A_{sn}^{Gg}] \longrightarrow A_{JI}^{Gg} = \sqrt{2}a_{ji}a_{ki} \quad \text{for } \begin{cases} J = 4, 5, 6; (j, k) = (2, 3), (1, 3), (1, 2) \\ I = 1, 2, 3; i = 1, 2, 3 \end{cases} \quad (32)$$

$$[A_{ss}^{Gg}] \longrightarrow A_{IJ}^{Gg} = a_{im}a_{kn} + a_{in}a_{km} \quad \text{for} \quad \begin{cases} I = 4, 5, 6; (i, k) = (2, 3), (1, 3), (1, 2) \\ J = 4, 5, 6; (m, n) = (2, 3), (1, 3), (1, 2) \end{cases} \quad (33)$$

The inverse of an orthogonal rotation matrix is given by its transpose. Both $[A^{Gg}]$ and $[a^{Gg}]$ are orthogonal rotation matrices and therefore have the following useful properties:

$$[A^{gG}] = [A^{Gg}]^t = [A^{Gg}]^{-1}, \quad [a^{gG}] = [a^{Gg}]^t = [a^{Gg}]^{-1}, \quad (34)$$

where the transpose of $[A^{Gg}]$ is denoted by $[A^{gG}]$ and similarly of $[a^{Gg}]$.

4.3.2 Moduli Transformations

Components of the second Piola-Kirchhoff stress and electric displacement are calculated using the following Voigt-Mandel representation for a piezoelectric constitutive model using

$$\{T^g\} = [\tilde{C}^g]\{S^g\} - [\tilde{e}^g]^t\{\mathcal{E}^g\}, \quad \{\mathcal{D}^g\} = [\tilde{e}^g]\{S^g\} + [\mathcal{K}^g]\{\mathcal{E}^g\}, \quad (35)$$

where superscripts g denote moduli, vector, and tensor components with respect to the material axes. If $\{T^g\}$ and $\{\mathcal{D}^g\}$ are pre-multiplied by the transformation matrices $[A^{gG}]$ and $[a^{gG}]$ respectively, then stress and electric displacement components will be converted to components with respect to user defined coordinate axes \mathbf{G} . However, this form is inconvenient in the constitutive model evaluation because the right hand side strain and electric field components are still expressed with respect to the material coordinate axes \mathbf{g} . Therefore, the strain and electric field components are expressed with respect to user defined coordinate axes as

$$\{S^g\} = [A^{gG}]\{S^G\}, \quad \{\mathcal{E}^g\} = [a^{gG}]\{\mathcal{E}^G\}. \quad (36)$$

Using (35) and (36) leads to transformation relations for elastic, piezoelectric, and permittivity matrices.

$$\begin{aligned} \{T^G\} &= [A^{Gg}]\{T^g\} \\ &= [A^{Gg}][\tilde{C}^g]\{S^g\} - [A^{Gg}][\tilde{e}^g]^t\{\mathcal{E}^g\} \\ &= \underbrace{[A^{Gg}][\tilde{C}^g][A^{gG}]}_{[\tilde{C}^G]}\{S^G\} - \underbrace{[A^{Gg}][\tilde{e}^g]^t[a^{gG}]}_{[\tilde{e}^G]^t}\{\mathcal{E}^G\} \end{aligned} \quad (37)$$

$$\begin{aligned} \{\mathcal{D}^G\} &= [a^{Gg}]\{\mathcal{D}^g\} \\ &= [a^{Gg}][\tilde{e}^g]\{S_m^g\} + [a^{Gg}][\mathcal{K}^g]\{\mathcal{E}^g\} \\ &= \underbrace{[a^{Gg}][\tilde{e}^g][A^{gG}]}_{[\tilde{e}^G]}\{S^G\} + \underbrace{[a^{Gg}][\mathcal{K}^g][a^{gG}]}_{[\mathcal{K}^G]}\{\mathcal{E}^G\} \end{aligned} \quad (38)$$

Note the piezoelectric matrix is consistently transformed in the above two equations for $\{T^G\}$ and $\{\mathcal{D}^G\}$.

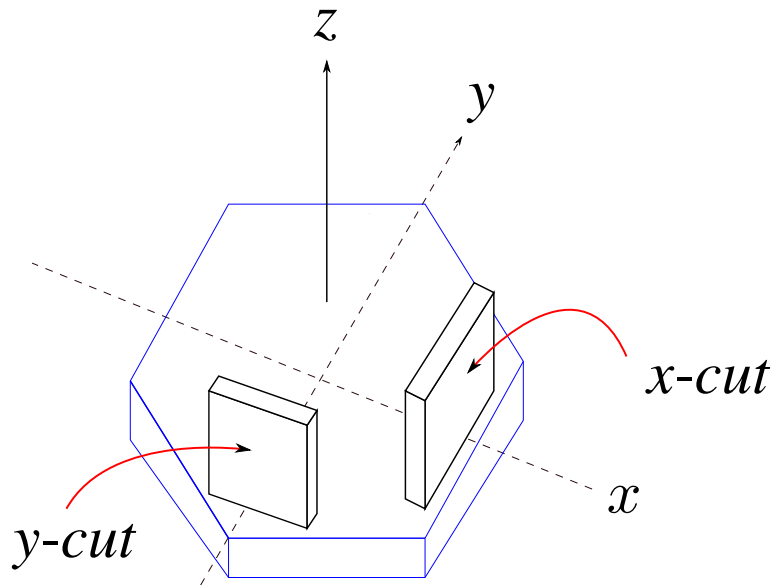


Figure 2. Sketch of quartz prism indicating orientation of x and y cuts; z axis is often referred to as the optical axis.

4.4 Moduli Transformations: Example

By way of example, this section demonstrates the transformations developed in the previous section.

Quartz is the canonical piezoelectric material. Properties for quartz and its various cuts are published and well known. In this section, a reference set of properties for y -cut quartz are given. Subsequently, these properties are transformed to a coordinate system known as AT -cut. This can then serve as a verification problem for computer implementation of the transformations discussed above.

4.4.1 Properties of y -cut Quartz

It is helpful to think of a piece of uncut quartz as a hexagonal prism – see Figure 2. Material axes are depicted in the graphic as x , y and z ; common samples of quartz are x -cuts and y -cuts. Note that both x -cut and y -cut quartz samples are associated with the principal axes and are merely rotated by 90° with respect to each other; these transformations do not introduce additional non-zero entries in material matrices.

There are 6 independent elastic moduli for quartz. With respect to y -cut quartz, the independent Voight elastic moduli are $C_{11}, C_{12}, C_{13}, C_{14}, C_{33}, C_{44}$. There are 2 independent piezoelectric moduli and 2 independent permittivity moduli. With respect to y -cut quartz, these independent moduli are e_{11}, e_{14} , and k_{11}, k_{33} respectively. Numerical values for these properties are given in Table 1. The

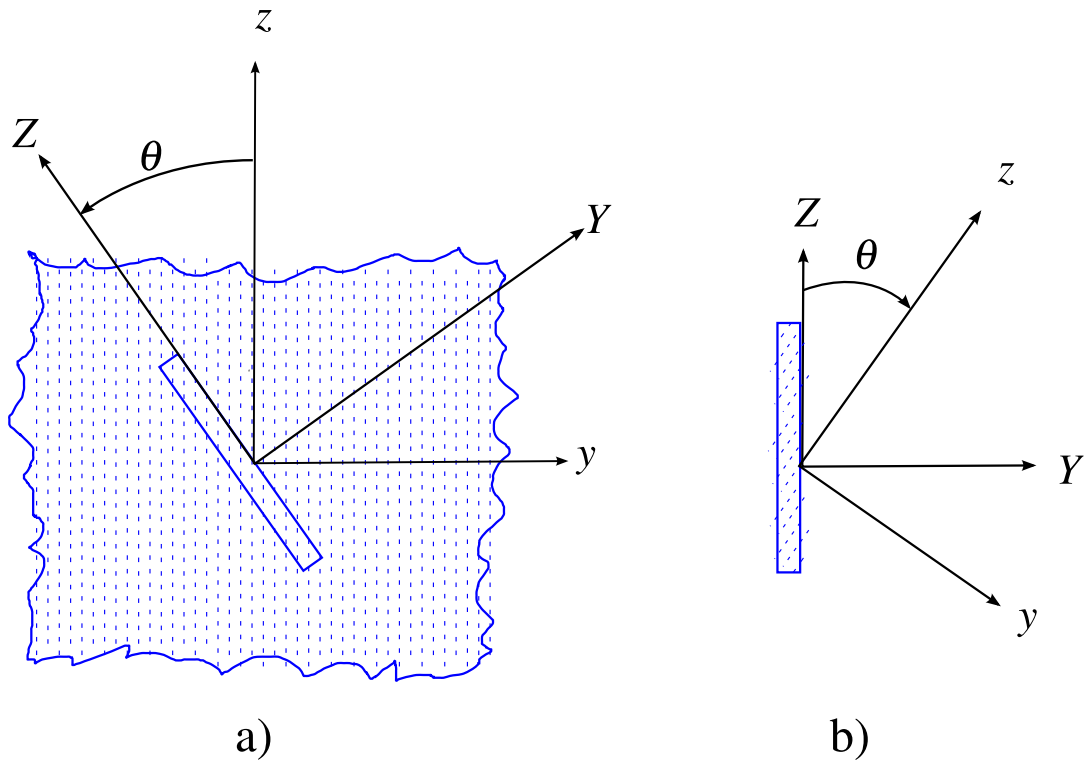


Figure 3. Schematic sketch of *y-cut* quartz; dotted lines indicate the optical *z*-axis; a) sample with respect to quartz prism; b) *AT-cut* sample: $\theta = 35.25^\circ$.

| | | | | | | | | |
|----------|----------------------|-----------------|----------|--------|-----------------------|----------|-------------------------|-----------------------------|
| C_{11} | 86.74×10^9 | $\frac{N}{m^2}$ | e_{11} | .171 | $\frac{Coulomb}{m^2}$ | k_{11} | 39.21×10^{-12} | $\frac{Coulomb}{V \cdot m}$ |
| C_{12} | 6.99×10^9 | | e_{14} | -.0406 | | k_{33} | 41.03×10^{-12} | |
| C_{13} | 11.91×10^9 | | | | | | | |
| C_{14} | -17.91×10^9 | | | | | | | |
| C_{33} | 107.2×10^9 | | | | | | | |
| C_{44} | 57.94×10^9 | | | | | | | |

Table 1. Voight representation of material properties for *y-cut* quartz [7].

structure of the Voight matrices for *y-cut* quartz is given below.

$$[C^g] = \begin{bmatrix} C_{11} & C_{12} & C_{13} & C_{14} & 0 & 0 \\ \text{symm} & C_{11} & C_{13} & -C_{14} & 0 & 0 \\ \text{symm} & \text{symm} & C_{33} & 0 & 0 & 0 \\ \text{symm} & \text{symm} & \text{symm} & C_{44} & 0 & 0 \\ \text{symm} & \text{symm} & \text{symm} & \text{symm} & C_{44} & 0 \\ \text{symm} & \text{symm} & \text{symm} & \text{symm} & \text{symm} & \frac{1}{2}(C_{11} - C_{12}) \end{bmatrix} \quad (39)$$

$$[e^g] = \begin{bmatrix} e_{11} & -e_{11} & 0 & e_{14} & 0 & 0 \\ 0 & 0 & 0 & 0 & -e_{14} & -e_{11} \\ 0 & 0 & 0 & 0 & 0 & 0 \end{bmatrix} \quad (40)$$

$$[\mathcal{K}^g] = \begin{bmatrix} k_{11} & 0 & 0 \\ 0 & k_{11} & 0 \\ 0 & 0 & k_{33} \end{bmatrix} \quad (41)$$

4.4.2 Transformation of *y-cut* Quartz to *AT-cut* Quartz

For verification, values for *y-cut* quartz in Table 1 are transformed into values for *AT-cut* quartz using the transformations in (37) and (38). Since the transformations described were developed for the Voight-Mandel representation, values for the Voight elastic and piezoelectric moduli in Table 1 must first be converted to the Voight-Mandel representation using the relations in (22) and (25). Then, using the orthogonality relations in (34), and the relationship between $[a^{Gg}]$ and $[A^{Gg}]$ using (30) thru (33), material properties for *AT-cut* quartz can be computed from properties for *y-cut* quartz. Note that after the transformation, properties are converted back to the Voight representation.

As shown in Figure 3, an *AT-cut* is a special version of *y-cut*. The relevant transformation matrices are given by identifying the *AT-cut* with a rotation of $\theta = -35.25^\circ$ about the x axis, see Figure 2 and Figure 3. To that end, rows of $[a^{gG}]$ express the material bases with respect to the problem coordinate bases. If $\hat{i}, \hat{j}, \hat{k}$, and $\hat{I}, \hat{J}, \hat{K}$ represent the material bases and the problem coordinates

bases respectively, then $[a^{sG}]$ is given by:

$$[a^{sG}] = \begin{bmatrix} 1 & 0 & 0 \\ 0 & \cos(\theta) & -\sin(\theta) \\ 0 & \sin(\theta) & \cos(\theta) \end{bmatrix}. \quad (42)$$

After transformation, the Voight representation of elastic, piezoelectric and permittivity moduli are given below for *AT-cut* quartz.

$$[C^G] = \begin{bmatrix} 86.74 & -8.25 & 27.15 & -3.66 & 0 & 0 \\ \text{symm} & 129.77 & -7.42 & 5.7 & 0 & 0 \\ \text{symm} & \text{symm} & 102.83 & 9.92 & 0 & 0 \\ \text{symm} & \text{symm} & \text{symm} & 38.61 & 0 & 0 \\ \text{symm} & \text{symm} & \text{symm} & \text{symm} & 68.81 & 2.53 \\ \text{symm} & \text{symm} & \text{symm} & \text{symm} & \text{symm} & 29.01 \end{bmatrix} \times 10^9 \frac{N}{m^2}$$

$$[e^G] = \begin{bmatrix} .171 & -.152 & -.0187 & .067 & 0 & 0 \\ 0 & 0 & 0 & 0 & .108 & -.095 \\ 0 & 0 & 0 & 0 & -.0761 & .067 \end{bmatrix} \frac{\text{Coulomb}}{m^2}$$

$$[\mathcal{K}^G] = \begin{bmatrix} 39.21 & 0 & 0 \\ \text{symm} & 39.82 & .86 \\ \text{symm} & \text{symm} & 40.42 \end{bmatrix} \times 10^{-12} \frac{\text{Coulomb}}{V \cdot m}$$

5 Nonlinear Kinematics for Stress and Polarization Calculations in *ALEGRA-EMMA*

In this section, relations developed in Section 2 are used to describe kinematically consistent algorithms for advancing the state of dielectric constitutive models. These concepts are then used to construct a kinematically consistent algorithm for advancing the state of the piezoelectric model in *ALEGRA-EMMA*.

With respect to kinematics, it is important to make a clear distinction between current coordinates and un-deformed coordinates. Because nearly all of the fields used for *ALEGRA-EMMA* calculations involve derivatives, careful attention must be given to whether derivatives are with respect to spatial coordinates $x = (x_1, x_2, x_3)$ or material coordinates $X = (X_1, X_2, X_3)$. The deformation gradient (1) plays a key role in transforming quantities between spatial and material coordinates. The tensors and fields denoted in Table 2 are of particular importance in the evaluation of dielectric constitutive models. In general, it is nearly impossible to avoid one or more of these transformations because *ALEGRA-EMMA* solves Gauss's Law on the spatial coordinates while the dielectric

constitutive models typically evaluate tensors and fields with respect to material coordinates. In addition to stress, constitutive models are required to return components of the permittivity tensor with respect to the current coordinates. If the material response includes an induced polarization due to deformation, then that must also be returned with respect to the spatial coordinates.

| Quantity | Material Representation | Spatial Representation |
|-----------------------|-------------------------|--|
| strain | S | $\boldsymbol{\varepsilon} = F^{-t} S F^{-1}$ |
| stress | T | $\boldsymbol{\sigma} = F T F^t / J$ |
| electric field | \mathcal{E}^G | $E^G = F^{-t} \mathcal{E}^G$ |
| electric displacement | \mathcal{D}^G | $D^G = F \mathcal{D}^G / J$ |
| polarization | \mathcal{P}^G | $P^G = F \mathcal{P}^G / J$ |
| permittivity moduli | \mathcal{K}^G | $K^G = F \mathcal{K}^G F^t / J$ |

Table 2. Material/Spatial Representation of Tensors and Fields

5.1 Gauss's Law for Dielectric Materials in *ALEGRA-EMMA*

Before discussing the state update algorithm for piezoelectricity, it is helpful to further consider Gauss's law for dielectric materials. The report by Montgomery [3] summarizes Gauss's law but does not include a treatment of the kinematics for dielectric materials. This section is a brief summary of the equations associated with Gauss's law but with an emphasis on the relevant kinematics. The consistent treatment of kinematics is crucial in *ALEGRA-EMMA* where large deformations and or rotations are routine. Most of the fields and tensors used in this section are identified in Table 2.

With respect to the material coordinate system, Gauss's law can be written as

$$\nabla_X \cdot \mathcal{D}^G = 0,$$

where $\mathcal{D}^G = \varepsilon_0 J F^{-1} F^{-t} \mathcal{E}^G + \mathcal{P}^G$ denotes the electric displacement, and ε_0 denotes the vacuum permittivity. The polarization \mathcal{P}^G is assumed to be derivable [6, 7] from a free energy function ψ as $\mathcal{P}_i^G = -\frac{\partial \psi}{\partial \mathcal{E}_i^G}$. In *ALEGRA-EMMA*, the polarization \mathcal{P}^G abstractly defines a so-called mechanical polarization π^G in the following way:

$$\mathcal{P}^G = \mathcal{K}^G \mathcal{E}^G + \pi^G, \tag{43}$$

where \mathcal{P}^G is decomposed into two pieces; the first piece linearly depends upon the electric field while the second piece, π^G , represents everything else. \mathcal{P}^G is conceptually independent of the polarization mechanism, i.e., it could be the final polarization after a change in temperature (pyroelectric), or after a change in the electric field (piezoelectric/ferroelectric), or after a change in shape (deformation) [4]. Here, the focus is on polarization due to applied electric fields and

mechanical deformations. For example, an energy functional that characterizes piezoelectricity is

$$\Psi(S_{kl}^G, \mathcal{E}_k^G) = \frac{1}{2} C_{ijkl}^G S_{ij}^G S_{kl}^G - e_{ijk}^G \mathcal{E}_i^G S_{jk}^G - \frac{1}{2} \chi_{ij}^G \mathcal{E}_i^G \mathcal{E}_j^G, \quad (44)$$

where χ_{ij} denotes components of the electric susceptibility tensor. Using 44, the polarization of a piezoelectric material is

$$\mathcal{P}^G = (\chi + \epsilon_0 J F^{-1} F^{-t}) \mathcal{E}^G + e^G S^G = \mathcal{K}^G \mathcal{E}^G + \pi^G \quad (45)$$

where \mathcal{K}^G denotes and defines the permittivity tensor, and π^G denotes and defines the mechanical polarization for a piezoelectric material.

In *ALEGRA-EMMA*, Gauss's law is solved using the divergence operator $\nabla \cdot$ with respect to the current configuration; hence Gauss's law is written with respect to the spatial coordinates

$$\nabla \cdot D^G = 0, \quad D^G = K^G E^G + F \pi^G / J, \quad (46)$$

where K^G is given by the push of \mathcal{K}^G (see Table 2). This equation is further developed by expressing the electric field as the gradient of a scalar potential. Faraday's law for electrostatics $\nabla \times E^G = 0$, allows the electric field to be derived from a scalar potential ϕ as $E^G = -\nabla \phi$, where ϕ is a function defined on the current configuration. Combining (45) and (46) yields the following representation for the electric displacement in the current configuration.

$$D^G = -K^G \nabla \phi + F \pi^G / J. \quad (47)$$

Then Gauss's law for dielectric materials in the current configuration is given by

$$\nabla \cdot (K^G \nabla \phi) = \nabla \cdot (F \pi^G / J). \quad (48)$$

ALEGRA-EMMA solves (48) for the scalar potential function ϕ over a domain which may consist of multiple dielectric materials and conductors. Solution procedures are described by Montgomery [3].

Because of the above relationships, the *ALEGRA-EMMA* solver and operators place requirements on the kind (Lagrangian versus Eulerian) of input and output fields dielectric constitutive models must use. With respect to kinematics, (48) requires dielectric constitutive models to calculate and

return the permittivity tensor K^G and the mechanical polarization vector $F\pi^G/J$, both of which are with respect to the current configuration. Relatedly, the *ALEGRA-EMMA* solver computes the electric field $E^G = -\nabla\phi$ as an input to dielectric constitutive models. Dielectric constitutive models in *ALEGRA-EMMA* must conform to these requirements; otherwise, calculations involving large deformations and rotations will be in error. The practical application of these concepts is described in the following section.

5.2 State Update Algorithm for Piezoelectricity in *ALEGRA-EMMA*

In this section, kinematic results and procedures developed in Sections 3 and 5.1 are applied to the piezoelectric model. There are multiple ways to implement the piezoelectricity model. The approach taken here relates to interface requirements (inputs and outputs) for constitutive models in *ALEGRA-EMMA*.

The piezoelectric model implementation consists of a *setup* phase that is run only once at the start of a problem, and an ongoing *update state* computation that is run for each *ALEGRA-EMMA* time step. With this approach, material moduli are rotated into the *ALEGRA-EMMA* problem coordinates during *setup*; this is a one time computation that does not need to be repeated for each time step; however, results from this calculation are used during each *update state* and hence there is a significant computational advantage to performing the material model transformations during *setup*. Calculations performed during *update state* relate to pushing and pulling fields and tensors between un-deformed and current configurations. The following sections closely describe the *setup* and *update state* used in *ALEGRA-EMMA*.

5.2.1 Setup

Piezoelectric material orientation and properties are user input parameters represented by $[a^{sG}]$ and $[C^s]$, $[e^s]$ and $[\mathcal{K}^s]$ respectively. The *setup* phase rotates user input material properties into the problem coordinate system. This consists of the following three steps which produces elastic $[C^G]$, piezoelectric $[e^G]$, and permittivity $[\mathcal{K}^G]$ moduli, all with respect to the problem coordinate axes.

Scale User Input Moduli Using the decomposition of elastic moduli depicted in (16), and the relations (22) and (25), scale $[C^s]$ and $[e^s]$ from user input parameters to the Voight-Mandel representations $[\tilde{C}^s]$, $[\tilde{e}^s]$. This step is not required for $[\mathcal{K}^s]$.

$$[\tilde{C}^s] = \begin{bmatrix} [C_{nm}^s] & \sqrt{2} [C_{ns}^s] \\ \sqrt{2} [C_{ns}^s] & 2 [C_{ss}^s] \end{bmatrix}$$

$$[\tilde{e}^g] = \begin{bmatrix} e_{111}^g & e_{122}^g & e_{133}^g & \sqrt{2}e_{123}^g & \sqrt{2}e_{113}^g & \sqrt{2}e_{112}^g \\ e_{211}^g & e_{222}^g & e_{233}^g & \sqrt{2}e_{223}^g & \sqrt{2}e_{213}^g & \sqrt{2}e_{212}^g \\ e_{311}^g & e_{322}^g & e_{333}^g & \sqrt{2}e_{323}^g & \sqrt{2}e_{313}^g & \sqrt{2}e_{312}^g \end{bmatrix}$$

Transform Moduli Using (37) and (38), transform $[\tilde{C}^g]$, $[\tilde{e}^g]$, and $[\mathcal{K}^g]$ into the problem coordinate axes.

$$[\tilde{C}^G] = [A^{Gg}][\tilde{C}^g][A^{gG}]$$

$$[\tilde{e}^G] = [a^{Gg}][\tilde{e}^g][A^{gG}]$$

$$[\mathcal{K}^G] = [a^{Gg}][\mathcal{K}^g][a^{gG}]$$

Scale Transformed Moduli: Reverse First Step Back out values for $[C^G]$ and $[e^G]$ using the above values for $[\tilde{C}^G]$ and $[\tilde{e}^G]$.

$$[C^G] = \frac{1}{2} \begin{bmatrix} 2[\tilde{C}_{nm}^G] & \sqrt{2}[\tilde{C}_{ns}^G] \\ \sqrt{2}[\tilde{C}_{ns}^G] & [\tilde{C}_{ss}^G] \end{bmatrix}$$

$$[e^G] = \frac{1}{\sqrt{2}} \begin{bmatrix} \sqrt{2}\tilde{e}_{111}^G & \sqrt{2}\tilde{e}_{122}^G & \sqrt{2}\tilde{e}_{133}^G & \tilde{e}_{123}^G & \tilde{e}_{113}^G & \tilde{e}_{112}^G \\ \sqrt{2}\tilde{e}_{211}^G & \sqrt{2}\tilde{e}_{222}^G & \sqrt{2}\tilde{e}_{233}^G & \tilde{e}_{223}^G & \tilde{e}_{213}^G & \tilde{e}_{212}^G \\ \sqrt{2}\tilde{e}_{311}^G & \sqrt{2}\tilde{e}_{322}^G & \sqrt{2}\tilde{e}_{333}^G & \tilde{e}_{323}^G & \tilde{e}_{313}^G & \tilde{e}_{312}^G \end{bmatrix}$$

5.2.2 Update State

The deformation gradient F is denoted as a matrix $[F]$ when acting on 2nd order tensors and vectors as matrices of tensor components $[\cdot]$ and arrays of vector components $\{\cdot\}$ respectively. Otherwise it is denoted as an operator which acts on 2nd order tensors and vectors.

The *update state* calculation is done for every *ALEGRA-EMMA* time step. This is a material model function for which the material properties $[C^G]$, $[e^G]$, and $[\mathcal{K}^G]$ are given; note that these were computed in the *setup* phase. The *update state* function is expected to return the so-called unrotated Cauchy stress tensor $\sigma^u = R^t \sigma R$, the spatial mechanical polarization π^G , and the spatial permittivity tensor K^G . Inputs to this evaluation are the spatial electric E^G , and V and R from

the polar decomposition $F = VR$. Because the material model is defined for evaluation with the Green-Lagrange strain tensor and the Lagrangian electric field \mathcal{E}^G , multiple transformations are required. The following sequence of steps summarize the *update state* evaluation.

Compute Engineering Strain Given $F = VR$, extract components E_{IJ} of the Green-Lagrange strain tensor:

$$E_{IJ} \leftarrow \frac{1}{2} (F^t F - I),$$

where I denotes the 2nd order identity tensor. Compute engineering strain $\{S^G\}$.

$$\{S^G\} = \begin{Bmatrix} S_1 \\ S_2 \\ S_3 \\ S_4 \\ S_5 \\ S_6 \end{Bmatrix} = \begin{Bmatrix} E_{11} \\ E_{22} \\ E_{33} \\ 2E_{23} \\ 2E_{13} \\ 2E_{12} \end{Bmatrix}$$

Pull Electric Field Since the incoming electric field E^G is with respect to the current coordinates, it must be pulled to enable its use in the constitutive model evaluation.

$$\{\mathcal{E}^G\} = [F^t] \{E^G\}$$

Evaluate 2nd Piola Kirchhoff Stress Given components of the engineering strain $\{S^G\}$ and components of the Lagrangian electric field $\{\mathcal{E}^G\}$, components $\{T^G\}$ of the 2nd Piola Kirchhoff stress tensor are evaluated.

$$\{T^G\} = [C^G] \{S^G\} - [e^G]^t \{\mathcal{E}^G\}$$

Evaluate Mechanical Polarization The mechanical polarization π^G is computed by pushing $[e^G] \{S^G\}$

$$\{\pi^G\} = \frac{1}{J} [F] [e^G] \{S^G\},$$

where J is the determinant of $[F]$.

Compute Cauchy Stress This is a push of the 2nd Piola Kirchhoff stress tensor. Note that here, F and T^G denote proper operators as opposed to matrices of components.

$$\sigma = \frac{1}{J} F T^G F^t$$

De-rotate Cauchy Stress *ALEGRA-EMMA* expects the de-rotated Cauchy stress σ^u as an output from this function.

$$\sigma^u = R^t \sigma R,$$

where R is from the polar decomposition $F = VR$.

Push Permittivity Moduli *ALEGRA-EMMA* expects an output of the permittivity tensor with respect to the current coordinates.

$$[K^G] = \frac{1}{J} [F] \{ \mathcal{K}^G \} [F^t]$$

5.3 Examples

In this section, two simple examples are developed and documented. These are verification type problems for which inspection and study can be used to confirm correctness. Using the procedures and results from this report, expected solutions are developed and compared with those computed by *ALEGRA-EMMA*.

5.3.1 Rigid Rotation with Constant Electric Field

A constant electric field of magnitude E_y is applied to a thin slab of quartz by applying a voltage that varies linearly across the slab.

$$V(y) = V_0 - yE_y,$$

where y is a component of the current coordinates. While holding the above voltage, the slab is rigidly rotated about the x – *axis* and otherwise prevented from any distortion due to the piezoelectric effect; hence, all strains in the slab are zero. See Figure 4.

For this rotation, the current coordinates \mathbf{r} are expressed as a function of θ and the Lagrangian coordinates (X, Y, Z) .

$$\begin{aligned} \mathbf{r} &= x\hat{i} + y\hat{j} + z\hat{k} \\ &= X\hat{I} + (Y \cos(\theta) - Z \sin(\theta))\hat{J} + (Y \sin(\theta) + Z \cos(\theta))\hat{K}. \end{aligned}$$

Since there is no distortion of the material, the deformation gradient $F = R$, where R is the one-rotation operator.

$$[R] = \begin{bmatrix} 1 & 0 & 0 \\ 0 & \cos(\theta) & -\sin(\theta) \\ 0 & \sin(\theta) & \cos(\theta) \end{bmatrix}$$

The spatial electric field E is

$$\begin{aligned}
E &= -\frac{\partial V}{\partial y} \hat{j} = E_y \hat{j} \\
&= \langle E^g \rangle \{g\}, \\
&= E_y [\cos(\theta) \hat{J} + \sin(\theta) \hat{K}] \\
&= \langle E^G \rangle \{G\},
\end{aligned}$$

where $\{g\}$ denotes a column vector representation of the basis vectors $(\hat{i}, \hat{j}, \hat{k})$, and $\langle E^g \rangle$ denotes components of the electric field with respect to $\{g\}$; similarly, $\langle E^G \rangle$ denotes components of the electric field with respect to $\{G\}$.

Using the above vector components and matrices, components of the Lagrangian electric field $\mathcal{E} = F^t E = -F^t \nabla V$ for use in the constitutive model is evaluated.

$$\begin{aligned}
\{E^G\} &= [R] \{E^g\} \\
\{\mathcal{E}^G\} &= [F]^t \{E^G\} \\
&= [R]^t [R] \{E^g\} \\
&= \{E^g\}
\end{aligned}$$

Cauchy Stress Components It is expected that components of the Cauchy stress tensor evolve due to the rigid rotation. For example, at the end of a 90° rotation, σ_{xz} should take on the value of σ_{xy} from before the rotation; similarly, σ_{xy} should take on the negative of the value for σ_{xz} from before the rotation.

If the constitutive model for *y-cut* quartz is evaluated and then pushed, the exact values for $\sigma_{xz}(\theta)$ and $\sigma_{xy}(\theta)$ are found.

$$\sigma_{xy}(\theta) = E_y [-e_{11} \cos(\theta) + e_{14} \sin(\theta)]$$

$$\sigma_{xz}(\theta) = E_y [-e_{14} \cos(\theta) - e_{11} \sin(\theta)]$$

Permittivity Tensor Components As previously discussed, components of the permittivity tensor are pushed. Analytical values for elements of the permittivity tensor in the current configuration are given by

$$K_{xx}(\theta) = k_{11},$$

$$K_{yy}(\theta) = k_{11} \cos^2(\theta) + k_{33} \sin^2(\theta),$$

$$K_{yz}(\theta) = [k_{11} - k_{33}] \cos(\theta) \sin(\theta),$$

and

$$K_{zz}(\theta) = k_{33} \cos^2(\theta) + k_{11} \sin^2(\theta).$$

The above expressions for stress and permittivity components are compared with values computed using *ALEGRA-EMMA*; a plot is given in Figure 5. Note that values computed using *ALEGRA-EMMA* closely track the analytical values given above.

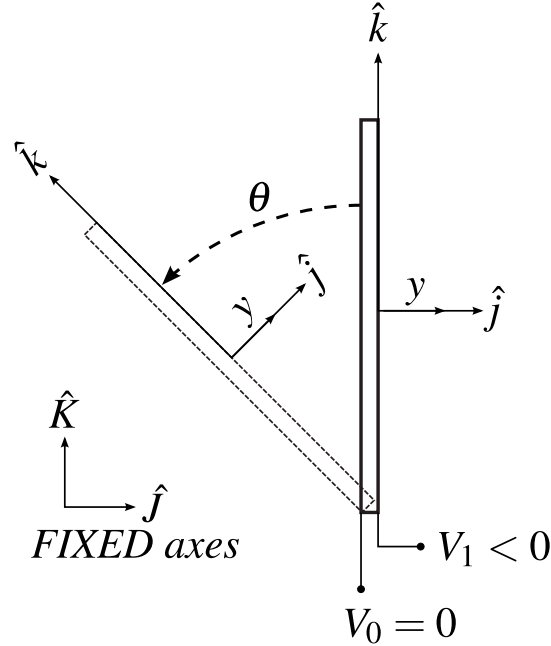


Figure 4. Rigid rotation with constant electric field. Material principal axes $\mathbf{g} \rightarrow (\hat{i}, \hat{j}, \hat{k})$ are initially aligned with the fixed global coordinate axes $\mathbf{G} \rightarrow (\hat{i}, \hat{j}, \hat{K})$.

5.3.2 Uniaxial Extension Plus Constant Electric Field Followed by Rigid Rotation

This example is closely related to the previous example. In addition to the voltage applied across the quartz slab, a constant state of uniaxial extension ϵ_{xx} is applied along the x -axis. A constant electric field of magnitude E_y is applied to a thin slab of quartz by applying a voltage that varies linearly across the slab.

$$V(y) = V_0 - yE_y,$$

where y is a component of the current coordinates. For this deformation and rotation, the current coordinates \mathbf{r} are expressed as a function of the uniaxial strain ϵ_{xx} , rotation θ , and the Lagrangian

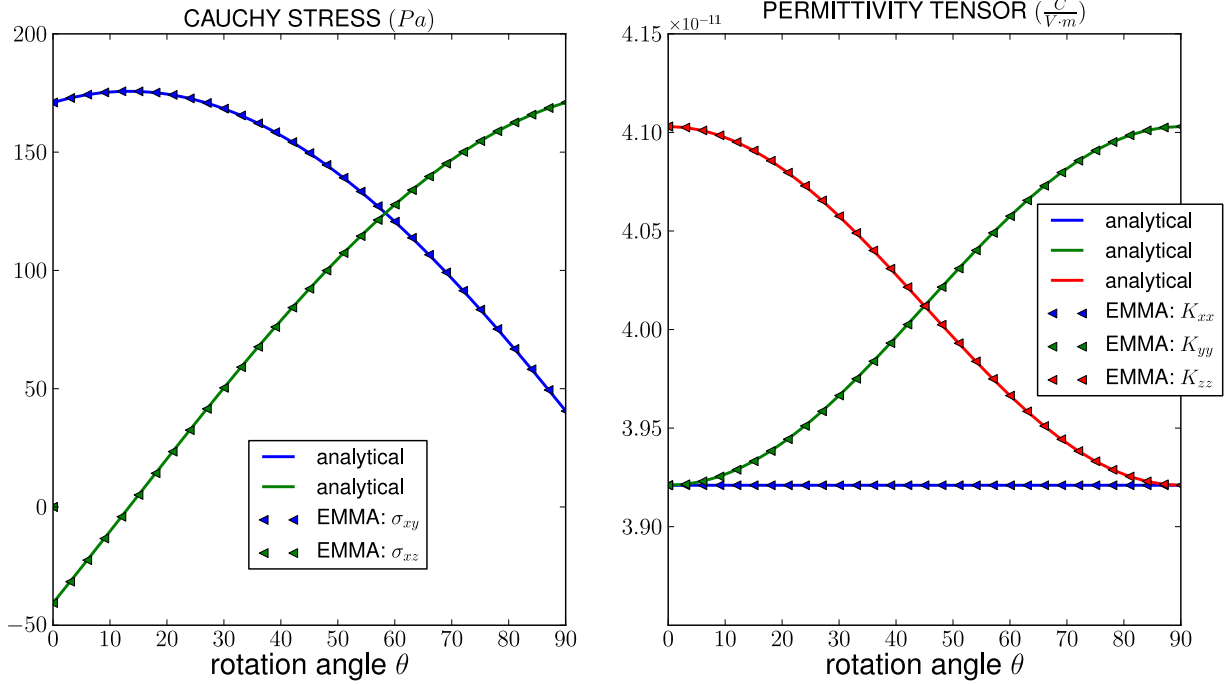


Figure 5. Example from Section 5.3.1. Rigid rotation of quartz slab with constant electric field. Stress and permittivity components. Material properties used are given in Table 1.

coordinates (X, Y, Z) .

$$\begin{aligned} \mathbf{r} &= x\hat{i} + y\hat{j} + z\hat{k} \\ &= X(1 + \varepsilon_{xx})\hat{I} + (Y \cos(\theta) - Z \sin(\theta))\hat{J} + (Y \sin(\theta) + Z \cos(\theta))\hat{K}. \end{aligned}$$

In this case, the deformation gradient F and rotation operator R are similar but not identical; components of F and R are:

$$[F] = \begin{bmatrix} 1 + \varepsilon_{xx} & 0 & 0 \\ 0 & \cos(\theta) & -\sin(\theta) \\ 0 & \sin(\theta) & \cos(\theta) \end{bmatrix}$$

$$[R] = \begin{bmatrix} 1 & 0 & 0 \\ 0 & \cos(\theta) & -\sin(\theta) \\ 0 & \sin(\theta) & \cos(\theta) \end{bmatrix}.$$

Proceeding along the same lines as the previous example, and following the procedures for *update state* described in Section 5.2.2, components of the Cauchy stress, permittivity, and mechanical polarization can be evaluated exactly. These values are given below.

Cauchy Stress Components After evaluating the Green-Lagrange strain tensor components and the electric field with respect to the reference configuration, the 2nd Piola Kirchhoff stress components are evaluated and subsequently pushed to give the Cauchy stress components.

$$\sigma_{xx}(\theta) = \frac{1}{2}C_{11}\epsilon_{xx}(1 + \epsilon_{xx})(2 + \epsilon_{xx})$$

$$\sigma_{xy}(\theta) = E_y[-e_{11} \cos(\theta) + e_{14} \sin(\theta)]$$

$$\sigma_{xz}(\theta) = E_y[-e_{14} \cos(\theta) + e_{11} \sin(\theta)]$$

$$\sigma_{yy}(\theta) = \frac{\epsilon_{xx}(2 + \epsilon_{xx})[C_{12} + C_{13} + (C_{12} - C_{13}) \cos(2\theta) - 2C_{14} \sin(2\theta)]}{4(1 + \epsilon_{xx})}$$

$$\sigma_{yz}(\theta) = \frac{\epsilon_{xx}(2 + \epsilon_{xx})[2C_{14} \cos(2\theta) + (C_{12} - C_{13}) \sin(2\theta)]}{4(1 + \epsilon_{xx})}$$

$$\sigma_{zz}(\theta) = \frac{\epsilon_{xx}(2 + \epsilon_{xx})[C_{12} + C_{13} + (-C_{12} + C_{13}) \cos(2\theta) + 2C_{14} \sin(2\theta)]}{4(1 + \epsilon_{xx})}$$

Permittivity Tensor Components Nonzero elements of the permittivity tensor with respect to the current coordinates are given.

$$K_{xx}(\theta) = (1 + \epsilon_{xx})k_{11}$$

$$K_{yy}(\theta) = \frac{k_{11} \cos^2(\theta) + k_{33} \sin^2(\theta)}{(1 + \epsilon_{xx})}$$

$$K_{yz}(\theta) = \frac{(k_{11} - k_{33}) \sin(2\theta)}{2(1 + \epsilon_{xx})}$$

$$K_{zz}(\theta) = \frac{k_{33} \cos^2(\theta) + k_{11} \sin^2(\theta)}{(1 + \epsilon_{xx})}$$

Mechanical polarization The uniaxial extension creates a constant mechanical polarization vector with only one non-zero component: P_x . In this case, the spatial and material representations are equivalent.

$$P_x(\theta) = \frac{1}{2}e_{11}\epsilon_{xx}(2 + \epsilon_{xx})$$

Plots of the Cauchy stress components and permittivity tensor components are given in Figures 6 and 7. Results computed using *ALEGRA-EMMA* closely track the analytical values developed above.

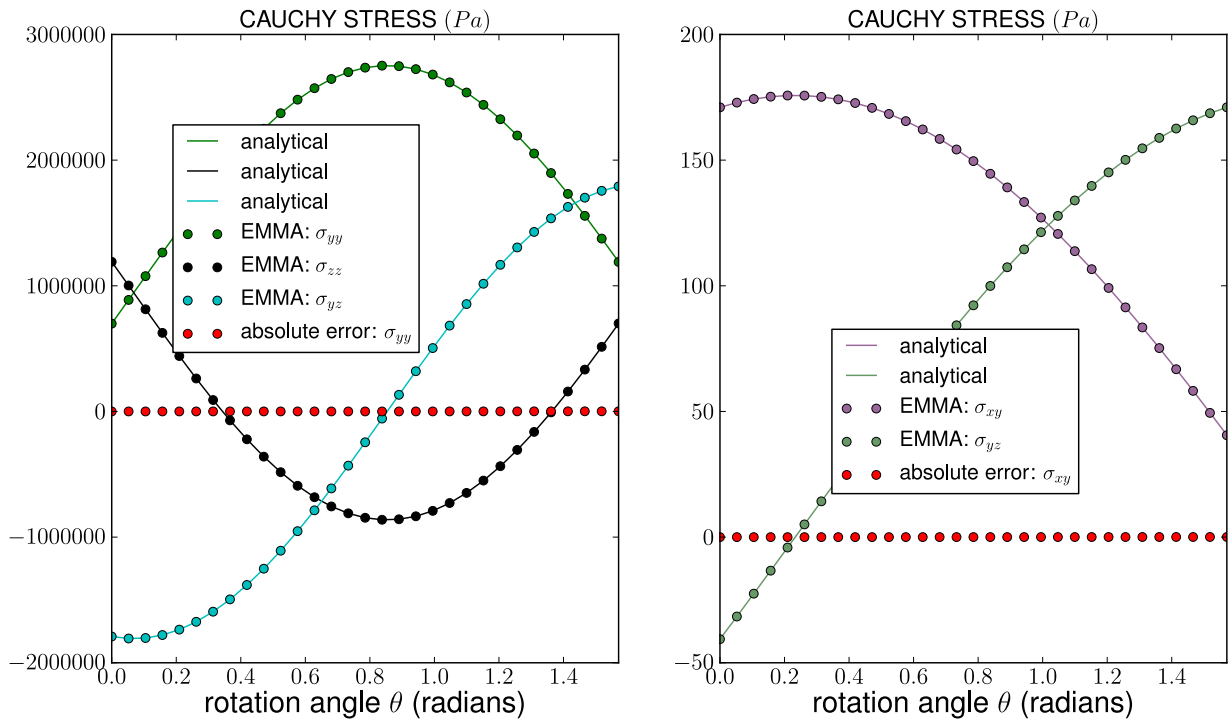


Figure 6. Example from Section 5.3.2. Uniaxial extension with constant electric field followed by rigid rotation. Cauchy stress. Material properties used are given in Table 1.

6 Summary

This report developed and documented nonlinear kinematics and material property transformations necessary for a consistent implementation of piezoelectric models in *ALEGRA-EMMA*. Important kinematics were established using Gauss's law and Faraday's law. Using these results, kinematically consistent constitutive model evaluations were developed and two examples demonstrating the kinematics were given. Required material property transformations were also developed and documented; one example was given.

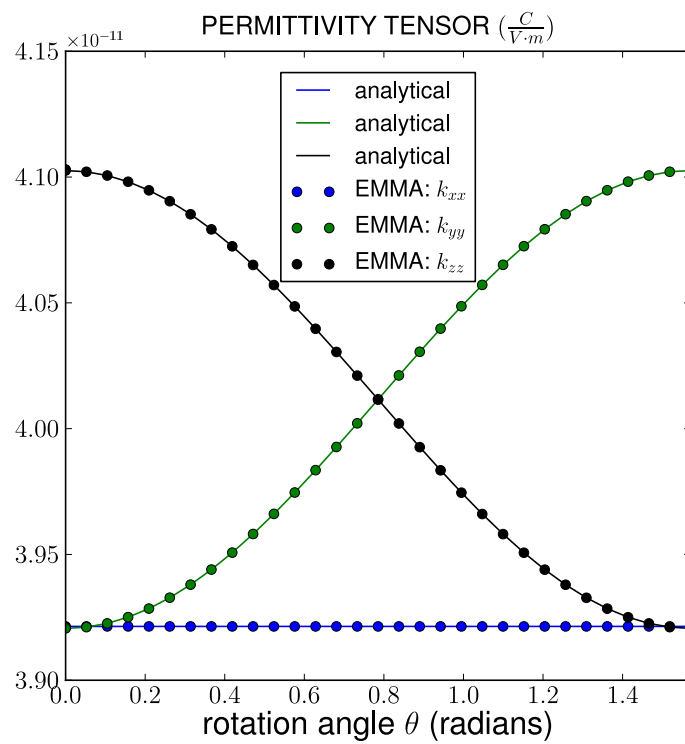


Figure 7. Example from Section 5.3.2. Uniaxial extension with constant electric field followed by rigid rotation. Permittivity tensor components with respect to current coordinates. Material properties used are given in Table 1.

References

- [1] Javier Bonet and Richard D. Wood. *Nonlinear continuum mechanics for finite element analysis*. Cambridge University Press, 1st edition, 1997.
- [2] David J. Griffiths. *Introduction to Electrodynamics*. Prentice Hall, 2nd edition, 1989.
- [3] Stephen T. Montgomery and Patrick F. Chavez. Basic equations and solution method for the calculation of the transient electromechanical response of dielectric devices. Technical Report SAND86-0755, Sandia National Laboratories, 1986.
- [4] J. F. Nye. *Physical Properties of Crystals*. Oxford University Press, 1985. reprinted 2010.
- [5] Allen C. Robinson and Michael K. Wong. Alegra-emma user manual (development draft). Technical Report SAND2011-draft, Sandia National Laboratories, 2011.
- [6] H. F. Tiersten. On the nonlinear equations of thermo-electroelasticity. *International Journal of Engineering Science*, 9:587–604, 1971.
- [7] Jashi Yang. *An introduction to the theory of piezoelectricity*. Springer, 2010.

DISTRIBUTION:

1 MS 0899 RIM-Reports Management, 9532 (electronic copy)



Sandia National Laboratories